RSC Advances

ROYAL SOCIETY OF CHEMISTRY

www.rsc.org/advances

Journal Name

RSCPublishing

ARTICLE

A Highly-sensitive Microfluidics System for Multiplexed Surface-enhanced Raman Scattering (SERS) Detection Based on Ag Nanodot Arrays

Cite this: DOI: 10.1039/x0xx00000x

Received 00th January 2012,
Accepted 00th January 2012

DOI: 10.1039/x0xx00000x

www.rsc.org/

Gang Chen[a,b,†], Yuyang Wang[a,†], Hailong Wang[a], Ming Cong[a], Lei Chen[a,d], Yongan Yang[c], Yijia Geng[a,d], Haibo Li[a], Shuping Xu[a] and Weiqing Xu[a,*]

We report a method to fabricate a highly-sensitive microfluidic surface-enhanced Raman scattering (SERS) chip with highly ordered Ag nanodot arrays as an enhancement substrate for the detection of multiplexed low-concentration analytes. The microfluidic SERS chip features a highly-ordered Ag nanodots array on quartz slides fabricated by depositing Ag with an ultrathin anodic aluminium oxide (AAO) film as a template, and a channel-patterned polydimethylsiloxane (PDMS) cover on top, allowing a gigantic enhancement of electromagnetic field in the proximity of the chip surface because of the localized surface plasmon resonance (LSPR) of the Ag nanodots. Via the utilization of a self-built SERS microspectrometer with an inverted configuration (Rev. Sci. Instrum., 2013, 84, 056105.), the multiplexed SERS signals of low concentration adenine and thiram can be readily detected with a detection limit down to 5.0×10^{-7}M. This detection system that we developed is flexible and have potentials for real commercialization.

1. Introduction.

For the recent decades, microfluidic technology has been developing rapidly because of its capabilities of performing safe, low-volume, low-energy-consuming, and high-throughput analytics, and has seen a revolution of miniaturized analytical laboratory equipments in the field of biology, chemistry and environment.[1,2] Methods of detection are essential parts of microfluidic analytics since real-life applications call for various proper ways of analyzing samples of interest. The mainstream microfluidic methods of detection include laser-induced fluorescence spectroscopy, UV-vis spectroscopy, mass spectrometry, electrochemical analysis, and surface-enhanced Raman scattering (SERS), etc. Among these detection methods, SERS stands out as a unique fingerprint spectroscopy, different from the other spectroscopies that measure the collective properties of molecular samples.[3] When molecules are in the proximity of nanostructured metal surface, their intensity of Raman scattering can be greatly amplified because of enhanced electromagnetic (EM) field around the surface due to the localized surface plasmon resonance (LSPR), making SERS a highly sensitive detection method. Therefore, SERS peaks are often very sharp, and they are ideal candidates for multiplexed detections, i.e., the detection and separation of signals from several analytes in mixed solutions at the same time.[4–6]

Combined with SERS, microfluidic analytics can be a powerful tool. Microfluidic SERS detection methods include using microfluidic channels to contribute to the better mixing and dispersion of Ag colloids,[7,8] using micro-droplets-based fluidic systems to produce SERS-active substrate and achieve uniform signals,[9] enriching analytes in microfluidic channels for detection,[10] and fabricating nano-patterned SERS substrates inside the microfluidic channels for high sensitivity and reproducibility, among which nano-patterned SERS substrates stand out as a more tunable approach to realize the excellent functions of microfluidic analytics. Sun et al reported that a femtosecond laser direct writing had been adopted for growing Ag nanoparticles SERS array in microfluidic channels with highly localizability and controllability for the on-line analysis of molecules.[11] Innocenzi et al fabricated mesoporous nanocomposite materials through the integration of the evaporation-induced self-assembly and the deep X-ray lithography, and micro-patterned films made using a mesoporous ordered silica matrix which contained Ag nanoparticles had been obtained.[12] Wu et al fabricated highly

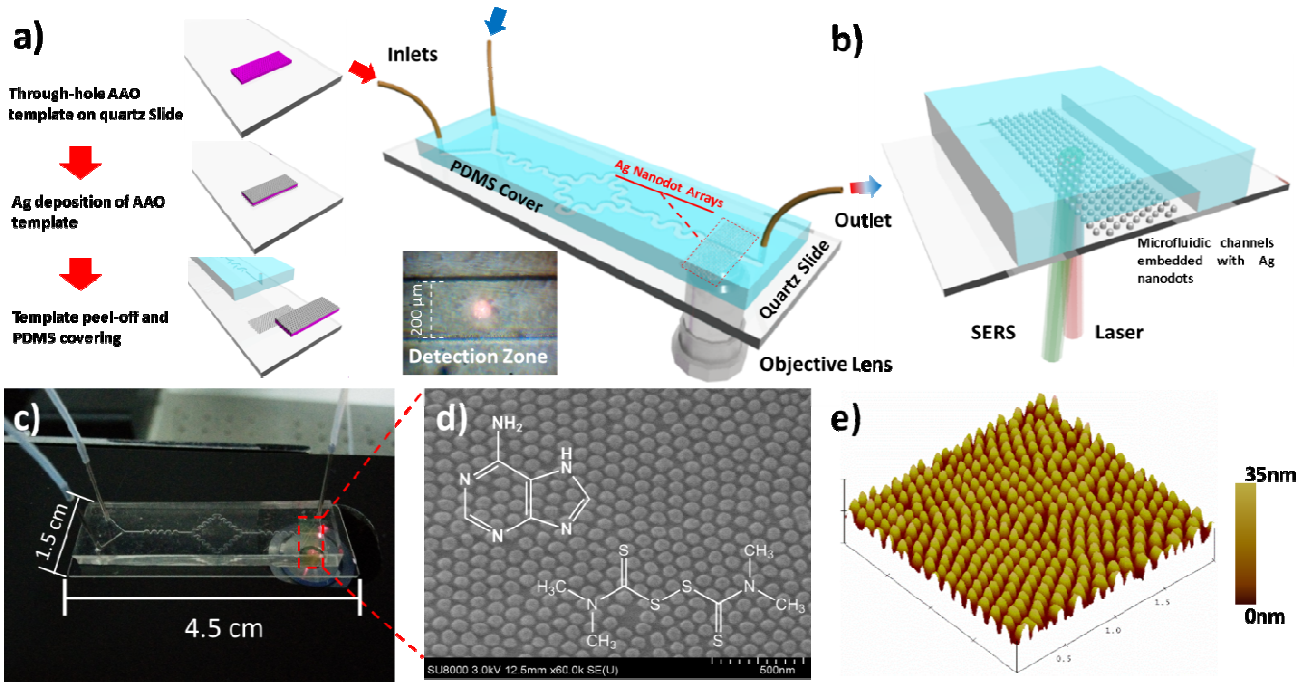

Scheme 1. a) Illustration of the fabrication of the microfluidic SERS chip based on Ag nanodot arrays, showing the completed chip configuration for final detection and a photo of the microfluidic SERS analyser during SERS collection. b) A magnified view illustrating the detailed configuration of the SERS chip. The scale is not real for illustration. c) Real image of the SERS chip mounted on the Raman analyser. d) SEM image of the Ag nanodots. e) The 3D atomic force microscopy (AFM) profile of the Ag nanodots.

roughened nano-pillar forests by etching photoresists as a template for a patterned noble metal SERS substrate in detection zones of a microfluidic channel for highly sensitive detection.[13] These works have been focused on the integration of nano-patterned ordered noble metal nanostructures into microfluidic channels, but most of them suffered high cost and the difficulty of focusing lasers for effective SERS excitation.

In this paper, we developed a microfluidic SERS chip based on an ordered Ag nanodot array as a SERS enhancement substrate, together with an improvement of laser path for the efficient excitation and collection of SERS signals. The Ag nanodot array was evaporated on a quartz slide through a through-hole ultrathin anodic aluminium oxide (AAO) template and it was later sealed under the microfluidic channels as a detection zone. A polydimethylsiloxane (PDMS) cover with designed concave channels was mounted and bonded to the quartz slide with the nanodot array, and plastic tubes with diameters correspondent to the width of the channels were inserted as inlets and outlets on the PDMS cover, making a complete SERS microfluidic chip. By doing so, the Ag nanodot array as an enhancement substrate was encapsulated in an airtight SERS chip, enhancing its long-term stability and strengthening its resistance to friction and contaminations.

In addition to the fabrication of the SERS chip, we also cope with the current difficulty of focusing laser spots onto the SERS-active surface. Since current state-of-art SERS instruments mainly adopt the method of focusing the laser spots from the channel side (except the optical fibre sensor approach), making it very difficult for a SERS equipment with a common optical fibre probe to easily locate and focus the laser spot on the SERS-active sites due to its lack of a imaging system.[11,13–16] Nevertheless, it's even harder for a commercial Raman solution to focus inside the microfluidic channel because the existence of a polymer cover may contaminate the Raman signals of the analytes, and the circulation tubes may be too cumbersome for SERS detections. Therefore, we employed a self-developed Raman micro-analyser equipped with an inverted laser path and a XYZ-axis moveable microscopic imaging and detection system [17] for measuring this SERS chip microfluidic, realizing the easy focusing of laser spots and on-site, real-time SERS detections.

2. Results and Discussion.

Scheme 1(a) illustrates the procedures of the fabrication of the microfluidic chip and the setup of the detection system. A through-hole AAO film made by traditional two-step method was mounted on a quartz slide as reported by Lei et al.[18–20] The quartz slide was cleaned by a O_2 plasma cleaner before the mounting of AAO film. The film has to be in the right place for the subsequent detection zone. Then an Ag layer was evaporated or sputtered onto the target AAO film. A part of Ag passed through the AAO template and reached the quartz slide to form an Ag nanodot array. The Ag layer left on the top of AAO template together with the AAO film was peeled off using a transparent tape, and a PDMS cover patterned with micro-channels was mounted and left to bond with the quartz slide, thus encapsulating the Ag nanodots on the bottom of the

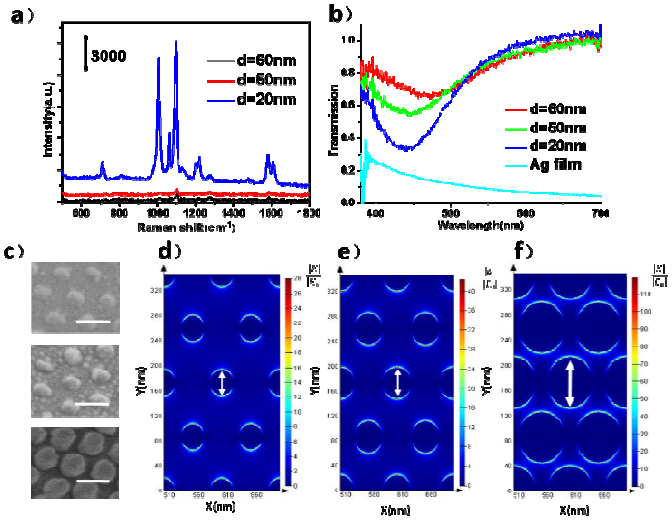

Fig.1 a) SERS spectra 4-MPycollected from substrates of Ag nanodot arrays with different dot-to-dot distances (d). b) LSPR spectra of the three Ag nanodot arrays with different d. c) SEM images of the three substrates. d), e) and f) are the simulated electric field distributions on the XY plane corresponding to d=60, 50 and 20 nm, respectively. Labeling of the gradient bar is contingent to calculation result and is not unified for clarification. The white arrows indicate the polarizing directions. The scale bar in c) represents 100 nm.

micro-channels. Before the bonding process, the PDMS have to be cleaned by O_2 plasma to ensure a good bonding effect. Then the inlets and the outlets were moulded to enable the circulation of analyte solutions, as in the example chip in Scheme 1, two inlets and one outlet were designed to take a two-component multiplexed detection. Curved channels ensure the better mixing of the two solutions, serving as the mixing zone, and the straight channels embedded with Ag nanodots serve as the detection zone. Scheme 1(b) shows the detailed configuration of the detection zone of the microfluidic chip. Subsequently the finished microfluidic chip was installed on a self-built Raman microspectrometer (Supra-1 model)[17] for SERS detections (Scheme 1(c)). Scheme 1(d) and (e) show the results of structure characterizations of Ag nanodots with a good uniformity.

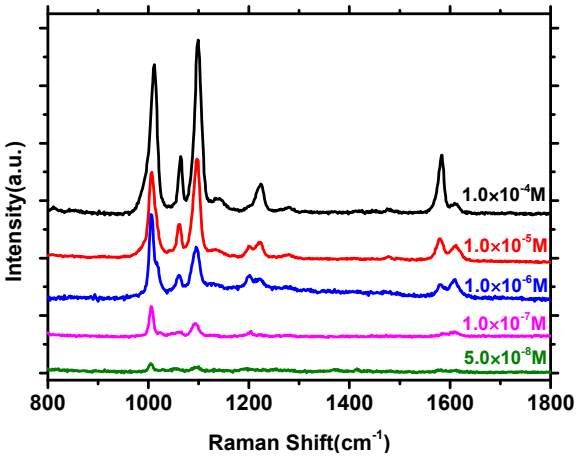

Fig. 2 SERS spectra of 4-Mpy with different concentrations detected by the micro-Raman analyser.

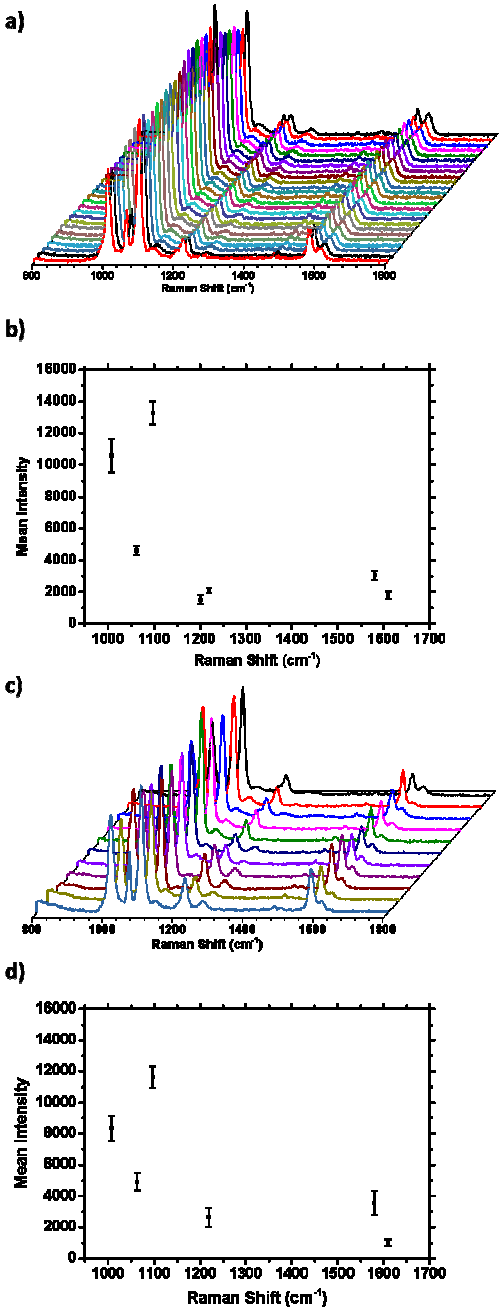

Fig. 3 a) SERS spectra of a 4-MPy solution (1.0×10^{-5} M) from 25 points randomly selected within a dried drop. b) Error bar graph of characteristic peaks of the 25 SERS spectra. c) 11 average SERS spectra of the 4-MPy solution (1.0×10^{-5} M) from 11 different Ag nanodot arrays respectively. Each spectrum was averaged by five spectra collected from randomly selected points on the substrate. d) Error bar graph of the mean intensity of characteristic 4-MPy SERS peaks from the 11 average spectra.

To evaluate the effects of the nanoscale morphology on SERS enhancement of the Ag nanodot array, the SERS spectra 4-mercaptopyridine (4-MPy) on three kinds of Ag nanodot arrays with different dot-to-dot gaps were directly collected. Since SERS enhancement is mainly contributed to LSPR due to its ability to generate highly-concentrated EM field and the LSPR property depends on metallic nano-gap structures, we fabricated

several nanodot arrays with different dot-to-dot gaps (gap size (d)=60, 50 and 20 nm) by controlling pore-widening time (t=45, 50 and 55 min) respectively to optimize the best-performance substrate. Fig. 1(a) is the SERS spectra of 4-MPy solution (1.0×10^{-5} M) measured on three kinds of nanodot arrays with their corresponding SEM images in Fig 1(c). SERS signal has been greatly enhanced when d is 20 nm, which is consistent with the current theory that stronger LSPR field is generated on the nanostructures with smaller nano-gap sizes.[21–26] Fig. 1(b) shows the LSPR extinction spectra of the three kinds of Ag nanodot arrays. Since quartz slides with nanodot arrays are visibly transparent, LSPR extinction spectra were measured in the transmission mode. An evident blue-shift of LSRP peak wavelength (λ_{LSPR}) and a decreasing trend of transmission intensity (T) smaller that of Ag film can be observed with d decreasing. Finite-difference time-domain (FDTD) simulations
of the three kinds of substrates were conducted to explore the EM enhancement (CAD models for FDTD simulation can be found in ESI file). The origin of the blue-shift should be covered by two aspects: the dipolar plasmon resonance of the individual Ag nanoparticle and the coupling dipolar moments of the neighbouring nanodots. The simulation results show that the 20 nm-gap between the Ag nanodots (Fig 1(f)), although bigger than the usually proposed gap size of sub-10 nm with strong EM-concentrated ability, are still vital for strong EM field coupling and good SERS-active performance.

For the demonstration of SERS performance of the Ag nanodot arrays with optimized morphologies, 4-MPy solutions at different concentrations (1.0×10^{-4} ~ 1.0×10^{-8} M) were used for testing the enhancement ability and the signal reproducibility of the Ag nanodot array with d=20 nm. One droplet of the solution with a volume of 5.0 μL was dropped on the optimized substrate and left to dry before SERS collection. Fig 2 shows the concentration-dependent SERS spectra of 4-MPy, demonstrating a detection limit of 1.0×10^{-8} M. For a SERS substrate of decent performance, reproducibility has to be considered as an important issue. Therefore, SERS signals on 25 points on an area of 2 mm^2 were collected as shown in Fig. 3(a). The error bar graph is shown in Fig. 3(b), showing the biggest relative standard deviation of 10.2% at 1097cm^{-1}, which meets the criteria of a high-performance SERS substrate.[27,28] Also, the batch-to-batch reproducibility of the Ag nanodot array substrates was evaluated by randomly collecting SERS signals of a 4-MPy solution (1.0×10^{-5} M) from 11 different substrates. Shown in Fig. 3(c) is the average spectra of the SERS signals collected respectively from the 11 different substrates. Fig. 3(d) shows

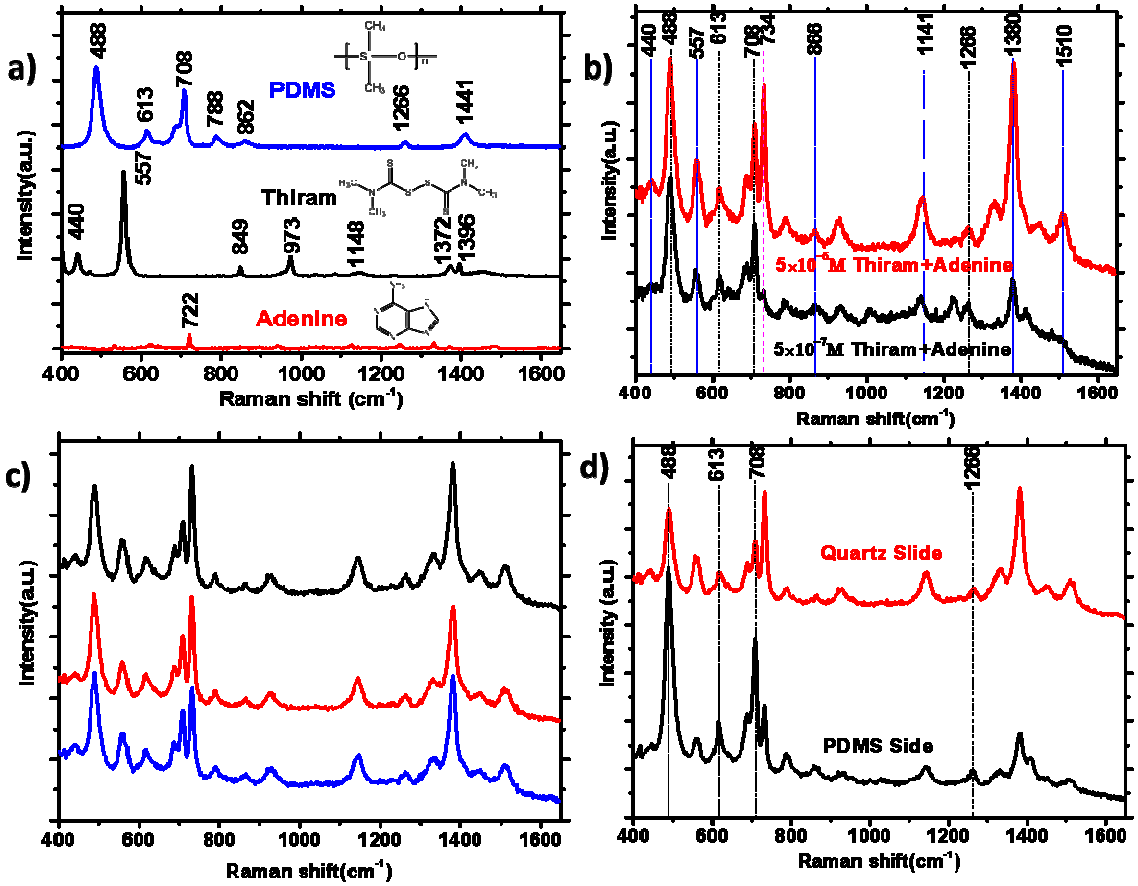

Fig 4. a) Normal Raman spectrum of PDMS cover and powder Raman scatterings of thiram and adenine. b) SERS spectra of two mixture solution of 5.0×10^{-7}M and 5.0×10^{-6}M thiram and adenine injected into the SERS chip channels. The pink dashed line represent the peaks of adenine, the black dash-dot-dot line the peaks of PDMS, and the blue dotted line the peaks of thiram. c) SERS spectra of the mixture solution collected from three different point in the detection zone. d) SERS spectra at the same spot collected from the quartz slide side and the PDMS side of the SERS chip.

the error bar graph of the average spectra, demonstrating relative standard deviations from 5.9% to 23.7% varying from peaks to peaks.

Therefore, the Ag nanodot array with an average gap size of 20 nm (corresponding diameter of 80 nm) and a height of 35 nm were used in the fabrication of the microfluidic enhancement substrate. It has to be noted that in the current Ag nanodot-based nanostructure, we cannot not render the SERS substrate a recyclable enhancement substrate, although which can be compensated by a multi-batch channel configuration.

The difference of a complete microfluidic SERS chip from a direct substrate is that a cumbersome PDMS cover with moulded channels is capped onto the Ag nanodot array. Therefore questions follow inevitably whether the enhancement substrate can retain the ability of SERS enhancement, and what should be the ideal way of collecting satisfactory SERS signals when the substrate is covered underneath the PDMS cover. Our research group has reported a micro-Raman analyser that copes with this problem in our previous publication.[17] The reported Raman micro-analyser integrates an inverted microscopic imaging system and a Raman detection system for Raman experiments, with a 3-axis stage controlled by step motors for easy positioning of the laser spot onto the detection zone. Furthermore, the optimized setup of the micro-Raman analyser was designed under the consideration of the microfluidic chips that are often capped with moulded channels, so the inverted micro-imaging system and the Raman system were under the microfluidic chips, minimizing the interference brought about by the cumbersome PDMS cover and circulation tubes, while in the meantime retaining SERS enhancement ability of the substrate during detections. In this paper, we utilized this Raman micro-analyser for SERS detections.

To evaluate the performance of the microfluidic SERS chip, the solutions of difference concentrations of adenine ($C_5H_5N_5$), a nucleobase in DNA series that have important roles in biochemistry, and thiram ($C_6H_{12}N_2S_4$), an ectoparasticide widely used in seeds and crops and an acute toxin, were injected through the two inlets simultaneously. Through the mixing zone, two solutions were well mixed into one analyte solution over the nanodot area before being flushed out through the outlet. A total of 10 μL solution was injected for each time of detection, which took 15 min for the analyte molecules to deposit evenly onto the Ag nanodots before Raman detections. It should be noted that for molecules like thiram and adenine which have no thiols or other functional groups that can make them easily bond to the surface of the plasmonic metal surface, it is normally difficult to simply make a drop of the solution dried on the substrate then be able to complete the SERS detection, since the molecules will majorly locate in the peripheral region of the deposit due to the capillary forces near contact line, which is similar to the "coffee ring" effect, leading to a poor spatial reproducibility of SERS signal.[29,30] To inject a low-volume of the molecule solution in a microfluidic channel and let the molecules deposit evenly on the enhancement substrate before drying out the solution proves to be an ideal way of solving the problem. Fig. 4 (a) shows the Raman spectra of the PDMS polymer used in the chip, thiram and adenine powders, exposing the characteristic peaks of three substances without an enhancement substrate. Although the peak positions can be varied if the molecules are in the close range of or absorbed onto a plasmonic matrix, generating shifted Raman peaks, the powder Raman spectra of the target molecules are still necessary since they can provide us all of the fingerprint information or vibrational modes we need in the analysis of SERS signals in multiplexed SERS detections. Moreover, the PDMS cover didn't directly contact the Ag nanodot array in the detection (Scheme 1), so the Raman peaks should be consistent in the SERS characterization of the microfluidic SERS chip, which was exactly what was observed. Raman peaks of PDMS at 488 cm^{-1} (Si-O-Si stretching), 613 cm^{-1}, 708 cm^{-1} (Si-C symmetric stretching), 862 cm^{-1} (CH_3 symmetric rocking), 1266 cm^{-1} (CH_3 symmetric bending), and 1441 cm^{-1} (CH_3 asymmetric bending) are clearly observed in Fig. 4(a).[31] The above peaks are still observed without much change in peak position and intensity in the SERS spectra, demonstrating no PDMS cover was in direct contact with the Ag nanodots. As for thiram peaks, the medium strong 440 cm^{-2} (CH_3-NC deformation and C=S stretching) turned into a weak peak in the SERS spectra, the very strong 557 cm^{-1} (S-S stretching) peak turned into a medium strong one, the medium 849 cm^{-1} (CH_3-N stretching) became a very weak one at 866 cm^{-1}, the strong 973 cm^{-1} (C-S-S asymmetric stretching) disappeared, the weak 1148 cm^{-1} (CH_3 rocking and C-N stretching) turned into a medium strong one at 1141 cm^{-1}, the strong 1372 cm^{-1}(CH_3 symmetric deformation and C-N stretching) became a very strong one at 1380 cm^{-1}, the strong 1396 cm^{-1} (CH_3 symmetric deformation) peak disappeared, a new strong 1150 cm^{-1} (C-N stretching, CH_3 deformation, and CH_3 rocking) peak appeared (Fig.4(a)). For adenine peaks, the very strong 722 cm^{-1} (ring stretching) peak turned into a very strong 734 cm^{-1} peak, which is the only distinct characteristic peak of adenine (Fig. 4(a)). The very strong peaks of the adenine and thiram are demonstrated to be very sharp and distinct in SERS spectra collected with the Ag nanodot arrays as a result of enhancement, making multiplexed detection of two molecules viable.

Fig. 4(b) shows the spectra of adenine and thiram mixture solutions at the concentrations of 5.0×10^{-7}M and 5.0×10^{-6}M. The SERS characteristic peaks are evenly enhanced, and can be used to clearly identify both thiram and adenine due to the decent LSPR enhancement of the Ag nanodot array. In addition, three point throughout the detection zone with about a 2 mm length interval in the microchannel were chosen to collect the SERS signals of the mixture solution of 5.0×10^{-6}M. Fig. 4(c) shows good reproducibility throughout the three points, proving that the detection zone can be covered by the Ag nanodot arrays, enabling evenly distributed enhancement effects. Also, SERS signals collected from the PDMS side and quartz slide side respectively were compared in Fig. 4(d). As we have reported,[17] by focusing the laser spot from beneath the PDMS cover, there is a trade-off of the peak intensities between the SERS spectra collected from the quartz side (adopted configuration) and the PDMS side. When SERS is collected

from the PDMS side, the characteristic peaks of PDMS stand out as overwhelming signals, obscuring the peaks of the molecules, making multiplexed identification barely possible. When SERS is collected from the quartz side, the PDMS peaks can be observed not as the overwhelming signals, making the SERS peaks of the molecules distinct enough for low-concentration identification.

3. Experimental Section

Fabrication of the Ag nanodot arrays

An anodic aluminum oxide film was used as an evaporation mask for the fabrication of the nanodot arrays. First, an ultrapure aluminum (Al) sheet (99.999%) was cut into proper size and annealed in nitrogen ambience under 500 °C for 4 hours. Then the Al sheet was degreased in acetone, cleansed in water, and then the Al sheet was dipped into a 2.0×10^{-1}M NaOH solution for 3 min. Then the Al sheet was electropolished in a solution of $HClO_4$ and CH_3CH_2OH (V/V=2:5) for 1 min. Through a prior dip into NaOH, the electropolishing process can be shortened compared to a usual 2.5 min to acquire the same surface smoothness. After electropolishing, the Al sheet was set as the anode in a two-electrode electrochemical cell, with 3.0×10^{-1}M oxalic acid as the electrolyte and a Ti plate as the cathode. The voltage was 40V and the anodization period was 4 min. By now, a typical 300 nm AAO film connected to Al sheet was formed. Then a PMMA layer was spin-coated onto the AAO film, and annealed on a hot plate under 130 °C for 30 min. Then the Al base was removed in a $CuCl_2$ and HCl mixed solution, a PMMA-AAO transparent layer was acquired. Then the thin layer was floated on the surface of 5% H_3PO_4 solution to remove the barrier layer of the AAO. Then the PMMA-AAO layer was set on the surface of a quartz slide. The PMMA was later removed in acetone. A through-hole AAO layer with a thickness of 300 nm and pore diameter of 80 nm was formed on the quartz slide. Then, Ag layers with 35 nm was evaporated through AAO channels, and after removing the AAO layers together with Ag on the surface of AAO with a transparent tape, highly ordered Ag nanodot arrays were formed on quartz slide. SEM images were acquired using a field-emission scanning electron microscope (HITACHI SU8020). AFM images were collected from nanoscope IIIa scanning probe microscope from Digital Instruments 3100.

Fabrication of the microfluidic SERS chip

To fabricate a desired PDMS cover to compose a microfluidic channel with quartz substrate, a moulded SU-8 photoresist pattern on Si was built prior to the PDMS polymerization. SU-8 photoresist (from Wenhao Technology Co. Ltd.) was first spin-coated (1100 r/m) onto a clean Si substrate, and annealed under 65 °C for 5 min, and 95 °C for 30 min. After being exposed to a mercury lamp for 10 min, the SU-8 was annealed again for under 65 °C for 5 min, and under 95 °C for 12 min. Then the SU-8 layer was dipped in a SU-8 developer for 8 min until area that was not exposed to light be completely removed, leaving a SU-8 pattern with a 110 μm thickness. Then silicon substrate was silanized using trimethyl chlorosilane (TMSCL) for easy detachment of the PDMS mould. Then PDMS initiator and monomer (Momentive RTV615A) (volume ratio is 1:10) was poured onto the SU-8 pattern and left for polymerization for 25 min under 70 °C on a hot plate. After being detached from the SU-8 pattern, the PDMS cover with concave designed pattern was acquired. Then the PDMS mould was cleaned by O_2 plasma using a reactive-ion etching (RIE) machine (Oxford Instrument, PlasmaLab 80 Plus). Quartz slides were ultra-sonicated in DI water, ethanol and acetone in sequence, and then were cleaned by O_2 plasma cleaner. Then the quartz slides with the Ag nanodot arrays were used as the enhancement substrate of the SERS chip. First, Ag nanodot arrays were scratched with a scalpel to leave a regular region where the microfluidic channels are supposed to be. Then, the PDMS cover was bonded to the quartz slide for 12 hrs.

SERS detection

For the evaluation of the Ag nanodot arrays as a direct substrate, 4-MPy water solution with different concentrations was dropped and dried on the substrate before detection. In the SERS detection of thiram and adenine molecules in the SERS chip, a total of 10 μL of the mixture solution was injected to fill the microfluidic channels. Then the solution was left for 15 min for the molecules to settle down and deposit onto the Ag plasmonic substrate. The laser spot was focused in the channels of the detection zone covered by the Ag nanodots using an 10x objective lens (NA=0.25). The Raman excitation wavelength was 785 nm, and the focused power used in the experiment was measured to be 40 mW. This wavelength is chosen because of the fixed preset configuration of the home-made instrument.[17] Although the LSPR resonance of the substrate lies at about 500 nm, an excitation of 785 nm can already be enough to observe a decent enhancement, as confirmed in the FDTD simulation. The integration time in the 4-MPy detection was 5s, and in the SERS collection in the microfluidic chips, it was set to 10s. A freshly made Ag nanodot-based chip was used when the detection zone was exhausted by saturated laser illumination in the SERS detection.

FDTD Simulation

The 3D simulation was carried out to compute the electric field enhancement and distribution using the FDTD solution software from Lumerical.[32] CAD models of the three nanodot substrate can be found in ESI file. The Ag nanodot arrays are modelled as half-ellipsoidal nanoparticles arrayed in hexagonal geometries. The height of the Ag nanodot arrays are 35 nm throughout the simulation, and the diameters are 40 nm, 50 nm, 80 nm according to experimental practices. The optical constants of the materials were directly imported from Palik database.[33] Yee cell method was used in the calculation to match the need of the geometry. A 785 nm plane wave source polarized in Y direction perpendicular to X direction was used. The simulation region is X=200 nm, Y=346 nm, and Z=4 μm. The boundary conditions in the simulation is perfectly matched

layers for Z plane, symmetric for Y plane and anti-symmetric for X plane.

4. Conclusions

We designed and built a microfluidic SERS system featuring an enhancement substrate based on Ag nanodot arrays and an inverted Raman analyser. The highly ordered nanostructured substrate can provide reproducible SERS signals throughout the coverage of the nanodot arrays with decent enhancement effects, enabling the multiplexed SERS signal collection of thiram and adenine with concentrations as low as 5.0×10^{-7}M. Using the Raman micro-analyser with an inverted configuration, the signal interference brought about by the PDMS cover can be avoided. Our fabrication method of a microfluidic SERS system obviates the need of using high-cost nanofabrication machines. Further effort still needs to be going on to integrate more functional parts into the system, making it truly capable of real-life applications

Acknowledgements

This work was supported by National Instrumentation Program (NIP) of the Ministry of Science and Technology of China No. 2011YQ03012408, the National Natural Science Foundation of China NSFC Grant Nos. 21373096, 21073073 and 91027010 and Innovation Program of the State Key Laboratory of Supramolecular Structure and Materials..

Notes and references

[a] State Key laboratory of Supramolecular Structure and Materials, Institute of Theoretical Chemistry, Jilin University, 2699 Qianjin Ave., Changchun, The People's Republic of China.
[b] College of Chemistry, Jilin University, 2699 Ave., Changchun, The People's Republic of China.
[c] Department of Physics and Electronic Science, Chu Xiong Normal University, Chuxiong 675000, The People's Republic of China
[d] College of Physics, Jilin University, 2699 Ave., Changchun, The People's Republic of China
* To whom correspondence should be addressed. Email: xuwq@jlu.edu.cn
† These two authors contributed equally to this work and should be regarded as co-first authors.

Electronic Supplementary Information (ESI) available:1. CAD models for FDTD simulation. See DOI: 10.1039/b000000x/

1 Janasek, J. Franzke, and A. Manz, *Nature*, 2006, **442**, 374–380.
2 P. Yager, T. Edwards, E. Fu, K. Helton, K. Nelson, M. R. Tam, and B. H. Weigl, *Nature*, 2006, **442**, 412–418.
3 Y. Zhao, D. Chen, H. Yue, J. B. French, J. Rufo, S. J. Benkovic, and T. J. Huang, *Lab. Chip*, 2013, **13**, 2183.
4 J. A. Dougan and K. Faulds, *Analyst*, 2012, **137**, 545–554.
5 M. Fan, P. Wang, C. Escobedo, D. Sinton, and A. G. Brolo, *Lab. Chip*, 2012, **12**, 1554.
6 J. A. Ruemmele, W. P. Hall, L. K. Ruvuna, and R. P. Van Duyne, *Anal. Chem.*, 2013, **85**, 4560–4566.
7 L. X. Quang, C. Lim, G. H. Seong, J. Choo, K. J. Do, and S.-K. Yoo, *Lab. Chip*, 2008, **8**, 2214.
8 S. Lee, J. Choi, L. Chen, B. Park, J. B. Kyong, G. H. Seong, J. Choo, Y. Lee, K.-H. Shin, E. K. Lee, S.-W. Joo, and K.-H. Lee, *Anal. Chim. Acta*, 2007, **590**, 139–144.
9 A. März, T. Henkel, D. Cialla, M. Schmitt, and J. Popp, *Lab. Chip*, 2011, **11**, 3584.
10 P. C. Ashok, G. P. Singh, H. A. Rendall, T. F. Krauss, and K. Dholakia, *Lab. Chip*, 2011, **11**, 1262.
11 B.-B. Xu, Z.-C. Ma, L. Wang, R. Zhang, L.-G. Niu, Z. Yang, Y.-L. Zhang, W.-H. Zheng, B. Zhao, Y. Xu, Q.-D. Chen, H. Xia, and H.-B. Sun, *Lab. Chip*, 2011, **11**, 3347.
12 L. Malfatti, P. Falcaro, B. Marmiroli, H. Amenitsch, M. Piccinini, A. Falqui, and P. Innocenzi, *Nanoscale*, 2011, **3**, 3760.
13 H. Mao, W. Wu, D. She, G. Sun, P. Lv, and J. Xu, *Small*, 2014, **10**, 127–134.
14 M. P. Cecchini, J. Hong, C. Lim, J. Choo, T. Albrecht, A. J. deMello, and J. B. Edel, *Anal. Chem.*, 2011, **83**, 3076–3081.
15 X. Lu, D. R. Samuelson, Y. Xu, H. Zhang, S. Wang, B. A. Rasco, J. Xu, and M. E. Konkel, *Anal. Chem.*, 2013, **85**, 2320–2327.
16 B.-B. Xu, Y.-L. Zhang, H. Xia, W.-F. Dong, H. Ding, and H.-B. Sun, *Lab. Chip*, 2013, **13**, 1677.
17 H. Li, G. Chen, Y. Zhang, Y. Geng, Y. Gu, H. Wang, S. Xu, and W. Xu, *Rev. Sci. Instrum.*, 2013, **84**, 056105.
18 Y. Lei and W.-K. Chim, *Chem. Mater.*, 2005, **17**, 580–585.
19 Y. Lei, S. Yang, M. Wu, and G. Wilde, *Chem. Soc. Rev.*, 2011, **40**, 1247–1258.
20 Y. Lei, W. Cai, and G. Wilde, *Prog. Mater. Sci.*, 2007, **52**, 465–539.
21 S. J. Hurst, E. K. Payne, L. Qin, and C. A. Mirkin, *Angew. Chem. Int. Ed.*, 2006, **45**, 2672–2692.
22 L. Qin, S. Zou, C. Xue, A. Atkinson, G. C. Schatz, and C. A. Mirkin, *Proc. Natl. Acad. Sci.*, 2006, **103**, 13300–13303.
23 U. S. Dinish, F. C. Yaw, A. Agarwal, and M. Olivo, *Biosens. Bioelectron.*, 2011, **26**, 1987–1992.
24 M. Moskovits, *Nature*, 2011, **469**, 307–308.
25 H.-Y. Wu, C. J. Choi, and B. T. Cunningham, *Small*, 2012, **8**, 2878–2885.
26 Y. Gu, S. Xu, H. Li, S. Wang, M. Cong, J. R. Lombardi, and W. Xu, *J. Phys. Chem. Lett.*, 2013, **4**, 3153–3157.
27 M. J. Natan, *Faraday Discuss.*, 2006, **132**, 321.
28 B. Sharma, M. Fernanda Cardinal, S. L. Kleinman, N. G. Greeneltch, R. R. Frontiera, M. G. Blaber, G. C. Schatz, and R. P. Van Duyne, *MRS Bull.*, 2013, **38**, 615–624.
29 S. Choi, S. Stassi, A. P. Pisano, and T. I. Zohdi, *Langmuir*, 2010, **26**, 11690–11698.
30 W. Wang, Y. Yin, Z. Tan, and J. Liu, *Nanoscale*, 2014.
31 D. Cai, A. Neyer, R. Kuckuk, and H. M. Heise, *J. Mol. Struct.*, 2010, **976**, 274–281.
32 Https://www.lumerical.com
33 E. D. Palik, Ed., in *Handbook of Optical Constants of Solids*, Academic Press, Burlington, 1997, pp. 5–114.

We present a microfluidics system with Ag nanodot arrays as the enhancement substrate for multiplexed SERS detection of low-concentration mixture of thiram and adenine.

Gang Chen[a,b,†], Yuyang Wang[a,†], Hailong Wang[a], Ming Cong[a], Lei Chen[a], Yijia Geng[d], Haibo Li[a], Yongan Yang[c], Shuping Xu[a] and Weiqing Xu[a,*]

A Highly-sensitive Microfluidics System for Multiplexed Surface-enhanced Raman Scattering (SERS) Detection Based on Ag Nanodot Arrays

Keyword: SERS, anodic aluminum oxide, microfluidics, spectrometer, adenine, thiram

Toc Figure